

Flexible InGaZnO TFTs with f_{max} above 300 MHz

Niko Münzenrieder, *Member, IEEE*, Koichi Ishida, *Member, IEEE*, Tilo Meister, *Member, IEEE*, Giuseppe Cantarella, Luisa Petti, Corrado Carta, *Member, IEEE*, Frank Ellinger, *Senior Member, IEEE*, and Gerhard Tröster, *Senior Member, IEEE*

Abstract—In this letter, the AC performance and influence of bending on flexible IGZO thin-film transistors, exhibiting a maximum oscillation frequency (maximum power gain frequency) f_{max} beyond 300 MHz, are presented. Self-alignment was used to realize TFTs with channel length down to 0.5 μm . The layout of this TFTs was optimized for good AC performance. Besides the channel dimensions this includes ground-signal-ground contact pads. The AC performance of this short channel devices was evaluated by measuring their two port scattering parameters. These measurements were used to extract the unity gain power frequency from the maximum stable gain and the unilateral gain. The two complimentary definitions result in f_{max} values of (304 ± 12) MHz and (398 ± 53) MHz, respectively. Furthermore, the transistor performance is not significantly altered by mechanical strain. Here, f_{max} reduces by 3.6 % when a TFT is bent to a tensile radius of 3.5 mm.

Index Terms—Flexible electronics, Thin-film transistors, IGZO, Maximum oscillation frequency

I. INTRODUCTION

FLEXIBLE and stretchable devices operated in close proximity to the human body, or fabricated using roll-to-roll manufacturing techniques are considered one of the next major steps in the development of consumer electronics [1]. In this context, novel semiconductors, such as organic materials, amorphous silicon, and oxides attracted considerable attention. In particular amorphous Indium-Gallium-Zinc-Oxide (IGZO) [2] combines excellent electrical performance, with low temperature processability, and extreme bendability [3].

Besides the well investigated DC performance of such TFTs, their AC performance and in particular speed is important for circuits such as transmitters and amplifiers [4], [5]. In this context, rigid IGZO based ring oscillators demonstrated output frequencies of 880 kHz [6]. At the same time, flexible IGZO NFC circuits work with an externally generated 13.56 MHz clock signal [7], and flexible IGZO TFTs exhibited a transit frequency f_T of 135 MHz [8]. While ring oscillators allow measuring the stage delay of a large signal and f_T quantifies the unity current gain frequency, the maximum oscillation frequency f_{max} of a transistor is defined as its unity power

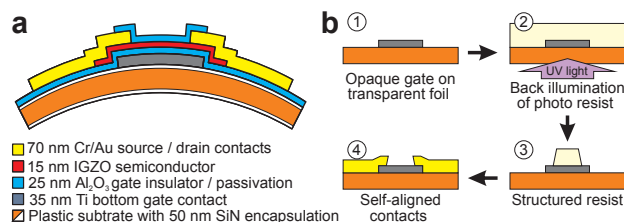


Fig. 1. a) Schematic and layer thicknesses of the flexible bottom gate inverted staggered IGZO TFTs. b) Fabrication process flow to manufacture self-aligned short channel TFTs on a polyimide substrate.

gain frequency [9]. Hence, this frequency is of paramount importance for the design of analog circuits.

Here, we show that the entirely flexible and self-aligned IGZO based TFTs presented in [8] can provide power gain at frequencies beyond 300 MHz even when the devices are bent. This is achieved by their short channel length of 0.5 μm in combination with a low gate capacitance of 15 pF, and a state of the art contact resistance of 12 Ωcm . This demonstrates that such a technology can be used to realize conformable and unobtrusive communication systems, based on high speed amplifiers circuits [10], for the future internet of things.

II. DEVICE STRUCTURE AND FABRICATION

The structure of the developed TFTs is shown in Fig. 1a. The devices were fabricated on free standing 50 μm thick polyimide foil using UV lithography. First, the substrate was encapsulated with 50 nm SiN (PECVD). Next, 35 nm thick Ti bottom gates were evaporated and structured by lift-off. The gate contacts were insulated by the ALD deposition of 25 nm Al₂O₃. This was done using a temperature of 150 $^{\circ}\text{C}$, which is the highest temperature in the fabrication process (i.e. there are no explicit annealing). Subsequently, 15 nm amorphous IGZO were RF sputtered using a ceramic InGaZnO₄ target. Both layers were structured by wet chemistry, using HCl:H₂O = 1:120 to etch IGZO, and HNO₃: H₃PO₄: CH₃COOH: H₂O = 1:25:5:5 to etch Al₂O₃. Next, the source and drain contacts were created using the self-alignment process illustrated in Fig. 1b. Here, the opaque gate on the partially transparent substrate acted as mask for positive AZ 4533 photo resist which was illuminated through the substrate (IGZO and Al₂O₃ layers are transparent). After development, a strip of photo resist is perfectly aligned to each gate. Subsequent to the following evaporation of a 10 nm Cr adhesion layer, and 60 nm of Au, this resist is used in a lift-off process to structure the TFT channel. Cr was chosen as adhesion layer because it can easily be etched, consequently, the channel width and contact pads are defined by wet etching using 50 g (NH₄)₂Ce(NO₃)₆

Manuscript received

N. Münzenrieder, K. Ishida, T. Meister contributed equally.

N. Münzenrieder, G. Cantarella, L. Petti, and G. Tröster are with the Institute for Electronics, ETH Zurich, 8092 Zurich, Switzerland.

K. Ishida, T. Meister, C. Carta, and F. Ellinger are with the Chair of Circuit Design and Network Theory, TU Dresden, 01069 Dresden, Germany.

L. Petti is also with the Faculty of Science and Technology, Free University of Bolzano-Bozen, 39100, Bolzano, Italy.

N. Münzenrieder is also with the Flexible Electronics Laboratory, Sensor Technology Research Centre, University of Sussex, Brighton, BN19QT, UK (corresponding email: n.s.munzenrieder@sussex.ac.uk)

This work was supported by the SNF, Switzerland, and DFG FFLexCom, Germany, through the project WISDOM, under Grant 200021E-160347/1.

+ 12 g CH_3COOH + 250 mL H_2O [Cr] and 15 g KI + 5 g I + 100 mL H_2O [Au]. The fabrication process is concluded by the deposition and structuring of an additional 25 nm thick Al_2O_3 layer as passivation. More information about the self-aligned fabrication can be found elsewhere [8]. Finally, it has to be mentioned that the employed self-alignment process enables the fabrication of devices on thermally and mechanically unstable flexible foils without the need for large tolerances.

III. RESULTS AND DISCUSSION

Fig. 2a shows a micrograph of a fully processed TFT. The corresponding SEM image in the inset confirms the channel length of $0.5\ \mu\text{m}$, and a gate to source/drain overlaps of $1.5\ \mu\text{m}$. These dimensions represent a trade-off between processability on free-standing plastic foils (large tolerances + lateral dimensions), high transconductance (short channels), current saturation (long TFT channels), low capacitance (small overlaps), and low contact resistance (large overlaps) [11]. They are the result of an optimization process involving test structures, characterization of TFTs with different channel length, as well as Comsol and Spice simulations [12]. The TFT layout comprises ground-signal-ground (GSG) contacts with a pitch size of $150\ \mu\text{m}$ to ensure reliable AC measurements. The visible sidewalls are due to the positive photoresist without undercut used for the channel lift-off, as well as the employed UV lamp and light scattering in the substrate which results in not perfectly collimated UV light. No significant influence of these sidewalls on f_{max} is expected, however it is assumed that a fully transparent substrate could reduce this sidewall effect. All TFTs were characterized under ambient conditions.

A. DC transistor performance

The TFTs were characterized using a Keysight B1500A parameter analyzer. The results are shown in Fig. 2b-d. This $0.5\ \mu\text{m}$ long TFT shows state of the art performance. A field effect mobility of $9\ \text{cm}^2\text{V}^{-1}\text{s}^{-1}$, a threshold voltage of $0\ \text{V}$, a subthreshold swing of $116\ \text{mV}/\text{dec}$, a maximum transconductance of $4.25\ \text{mS}/\text{cm}$, a maximum gate capacitance C_G of $15\ \text{pF}$, and an On/Off current ratio $>1 \times 10^8$ were extracted using the standard Shichman-Hodges model [13]. The frequency dependency of the gate capacitance in IGZO TFTs is attributed to the slow occupation of traps (RMS roughness of the Al_2O_3 -IGZO interface is $4.2\ \text{nm}$), parasitic resistances and slow response of free charges [8], [14]. This reduction of the C_G at high frequencies is an advantage for the AC performance. The gate leakage current always stays below $10\ \text{pA}$. However, it has to be mentioned that due to the extremely short channel some of the parameters are deteriorated. In particular the effective mobility is reduced by a contact resistances of $12\ \Omega\text{cm}$ (same order of magnitude as the channel resistance) [12]. Simultaneously, the output resistance is only $\approx 5.5\ \text{k}\Omega$ ($V_{GS} = 2\ \text{V}$). This is because of the low threshold voltage, and because the $0.5\ \mu\text{m}$ long TFT cannot be characterized in deep saturation (continuous drain-source voltages above $2\ \text{V}$ result in a permanent short circuit between the source and drain contacts). Since longer TFTs can withstand higher voltages, it can be concluded that the effective breakdown field of these

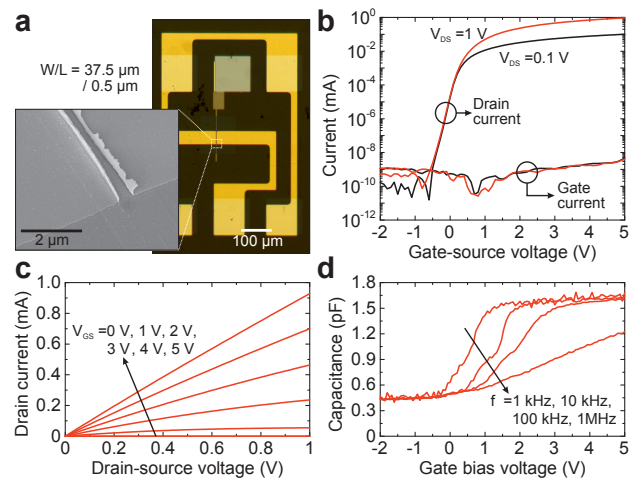


Fig. 2. a) Micrograph of a flexible IGZO TFT with a channel length of $0.5\ \mu\text{m}$ (the inset shows a SEM image of the channel region. Measured transfer characteristic (b), output characteristic (c), and gate capacitance (d) of a TFT with a W/L ratio of $37.5\ \mu\text{m}/0.5\ \mu\text{m}$.

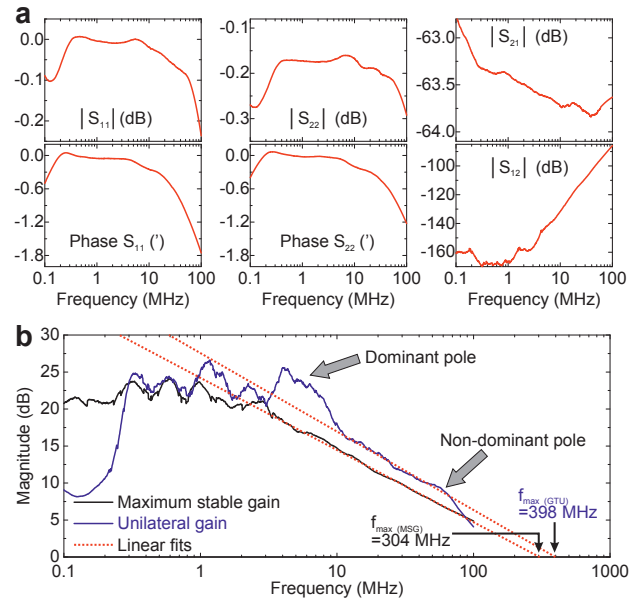


Fig. 3. a) Measured S-parameters of a TFT with a W/L ratio of $37.5\ \mu\text{m}/0.5\ \mu\text{m}$. The DC bias points were: $V_{DS} = 2\ \text{V}$, and $V_{GS} = 2\ \text{V}$. b) Maximum stable gain (Eq. 1) and unilateral gain (Eq. 2) calculated from S-parameters with resulting f_{max} .

IGZO channels is $<4\ \text{MV}/\text{m}$. This breakdown is also visible under the microscope. The limitation of the bias voltage has to be considered when designing circuits. At the same time, we like to mention that the demonstrated performance at low voltages shows that these TFTs can be used to realize flexible, low power and low voltage circuits.

B. Unity power gain frequency

The AC performance of the TFTs was characterized using a HP 8753E network analyzer. The DC bias points were $V_{DS} = 2\ \text{V}$, and $V_{GS} = 2\ \text{V}$. The resulting S-parameters for the same TFT as characterized in Fig. 2 are shown in Fig. 3a.

The maximum oscillation frequency of a transistor can be determined using multiple different definitions. Here, the two

most common one, corresponding to the unity gain frequencies of the maximum stable gain (MSG), and the unilateral gain (GTU) are used [15]. These parameters are calculated from the scattering parameters using the following equations [16]:

$$MSG = \frac{|S_{21}|}{|S_{12}|} \quad (1)$$

$$GTU = \frac{|S_{12}|^2}{(1 - |S_{11}|^2)(1 - |S_{22}|^2)} \quad (2)$$

Here S_{11} , S_{12} , S_{22} , S_{21} are the measured frequency dependent scattering parameters whereas port 1 was connected to the gate, and port 2 was connected to the drain. Fig. 3b illustrates the calculated MSG and GTU, as well as the resulting maximum oscillation frequencies. Whereas the MSG measurement shows a constant slope of -9.75 dB (close to the theoretical value of -10 dB), the GTU measurements exhibits multiple poles and is in general more noisy. The first and dominant pole is around 10 MHz, whereas the second pole around 60 MHz is non-dominant and only relevant for cascaded amplifiers. The slope after the dominant pole is -10.61 dB and hence also close to the theoretical value. As can be seen, both unity gain frequencies are above 300 MHz. The maximum stable gain results in a $f_{max(MSG)}$ of (304 ± 12) MHz and the unilateral gain results in a $f_{max(GTU)}$ of (398 ± 53) MHz. The given errors are calculated from the uncertainties of the linear fits which were obtained using the least square method.

The scaling of the measured f_{max} values for different channel length is illustrated in Fig. 4. Both, the MSG and GTU measurements show the expected behavior, namely a decrease of f_{max} in longer TFTs. This is also in line with corresponding transit frequency measurements [12]. In particular the GTU measurement also exhibits larger error bars at smaller frequencies. This is due to the general difficulty of performing S-parameter measurements at low frequencies.

Although these devices are currently the fastest flexible oxide TFTs [3], even higher frequencies of e.g. organic or oxide TFTs are desirable in the future. This calls for more aggressive scaling, including: planar nanoscale TFTs on plastic foils without deteriorated contact resistance (known from vertical TFTs [11]), electrostatic control of the channel, minimized parasitic resistances and capacities [12], control of the effective channel length reduction [17], and optimized overall ductility of flexible TFTs. This requires new techniques such as thinner layers to improve the pinch off behavior, self-alignment of additional layers to reduce parasitic capacities, or the use of plasma treatment and double gate structures to minimize the contact resistances [18], [19].

C. Bending

While the f_T and DC bending performance of flexible IGZO TFTs was already extensively investigated [3], [8], the presented TFTs were used to evaluate how f_{max} behaves under mechanical strain and bending to a radius of 3.5 mm. This was done by measuring the S-parameters while the TFT was bent. This induced tensile mechanical strain of 0.7% parallel to the TFT channel. The mechanical strain in the TFT channel

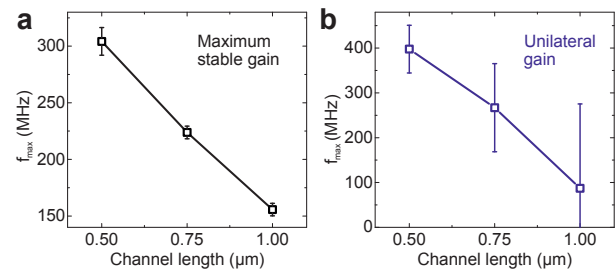


Fig. 4. Measured f_{max} extracted from maximum stable gain (a) and unilateral gain (b) for TFTs with different channel lengths.

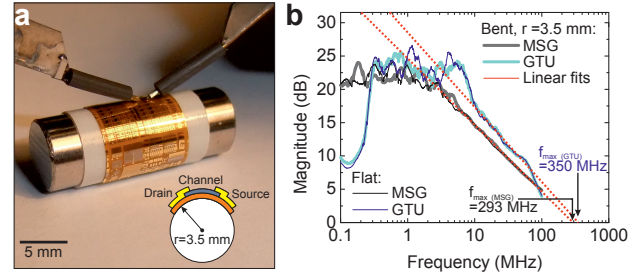


Fig. 5. a) Flexible TFT bent to a tensile radius of 3.5 mm, and contacted with GSG probes. b) Measured maximum stable gain, unilateral gain and f_{max} for a TFT with W/L ratio = $37.5 \mu\text{m}/0.5 \mu\text{m}$ while flat and while bent.

was calculated using the equation from [20]. Fig. 5a shows a photograph of the bend device. Reference measurements of the transfer characteristic showed that the bent TFTs exhibit performance parameter shifts expected for short flexible IGZO TFTs. Specifically a carrier mobility increase of 0.9%, and a threshold voltage decrease of 10 mV were extracted [8]. The resulting MSG and GTU measurements are shown in Fig. 5b. Here bending reduces $f_{max(MSG)}$ by 11.6 MHz and $f_{max(GTU)}$ by 47.7 MHz. Although this shifts are within the measurement uncertainty, a negative shift is expected. This is caused by the inverse dependency of f_{max} on the gate capacitance [16], and the increase of the gate capacitance of these TFTs under tensile stress. Tensile strain of 0.7% increases the measured C_G by 1.1% to 2.3%. This is due to the increased gate area and IGZO carrier concentration, and the reduced gate insulator thickness (Poisson effect) [21].

IV. CONCLUSION

The, to the very best of our knowledge, first characterization of the maximum oscillation frequency of flexible IGZO TFTs shows that entirely flexible technologies can be used to realize active transceivers operating in the Megahertz regime. The developed self-aligned transistors are fabricated on a free standing polyimide foil, exhibit a channel length down to $0.5 \mu\text{m}$, and stay fully functional even when exposed to tensile bending strain of 0.7%. S-parameter measurements were used to determine the unity gain frequency of the maximum stable gain, and the unilateral gain. Irrespectively of the chosen method, f_{max} was extracted to be >300 MHz. This extraction was one of the last missing parameters to fully describe the AC performance of flexible high speed IGZO TFTs.

REFERENCES

- [1] A. Nathan, A. Ahnood, M. T. Cole, S. Lee, Y. Suzuki, P. Hiralal, F. Bonaccorso, T. Hasan, L. Garcia-Gancedo, A. Dyadyusha, S. Haque, P. Andrew, S. Hofmann, J. Moultrie, D. Chu, A. J. Flewitt, A. C. Ferrari, M. J. Kelly, J. Robertson, G. A. J. Amaratunga, and W. I. Milne, "Flexible electronics: The next ubiquitous platform," *Proc. of the IEEE*, vol. 100, no. 13, pp. 1486–1517, 2012. <http://dx.doi.org/10.1109/JPROC.2012.2190168>
- [2] K. Nomura, H. Ohta, A. Takagi, T. Kamiya, M. Hirano, and H. Hosono, "Room-temperature fabrication of transparent flexible thin-film transistors using amorphous oxide semiconductors," *Nature*, vol. 432, no. 7016, pp. 488–492, 2004. <http://dx.doi.org/10.1038/nature03090>
- [3] L. Petti, N. Münzenrieder, C. Vogt, H. Faber, L. Büthe, G. Cantarella, F. Bottacchi, T. D. Anthopoulos, and G. Tröster, "Metal oxide semiconductor thin-film transistors for flexible electronics," *Applied Physics Reviews*, vol. 3, no. 2, p. 021303, 2016. <http://dx.doi.org/10.1063/1.4953034>
- [4] K. Myny, "The development of flexible integrated circuits based on thin-film transistors," *Nature Electronics*, vol. 1, no. 1, p. 30, 2018. <http://dx.doi.org/10.1038/s41928-017-0008-6>
- [5] R. Shabanpour, T. Meister, K. Ishida, B. Kheradmand-Boroujeni, C. Carta, F. Ellinger, L. Petti, N. Münzenrieder, G. A. Salvatore, and G. Tröster, "Design and analysis of high-gain amplifiers in flexible self-aligned a-igzo thin-film transistor technology," *Analog integrated circuits and signal processing*, vol. 87, no. 2, pp. 213–222, 2016. <https://doi.org/10.1007/s10470-015-0655-3>
- [6] Y. Guang, W. Chen-Fei, L. Hai, R. Fang-Fang, Z. Rong, Z. You-Dou, and H. Xiao-Ming, "Frequency performance of ring oscillators based on a-igzo thin-film transistors," *Chinese Physics Letters*, vol. 32, no. 4, p. 047302, 2015. <https://doi.org/10.1088/0256-307X/32/4/047302>
- [7] K. Myny, Y.-C. Lai, N. Papadopoulos, F. De Roose, M. Ameys, M. Willegems, S. Smout, S. Steudel, W. Dehaene, and J. Genoe, "15.2 a flexible iso14443-a compliant 7.5 mw 128b metal-oxide nfc barcode tag with direct clock division circuit from 13.56 mhz carrier," in *Solid-State Circuits Conference (ISSCC), 2017 IEEE International*. IEEE, 2017, pp. 258–259. <http://dx.doi.org/10.1109/ISSCC.2017.7870359>
- [8] N. Münzenrieder, L. Petti, C. Zysset, T. Kinkeldei, G. A. Salvatore, and G. Tröster, "Flexible self-aligned amorphous InGaZnO thin-film transistors with sub-micrometer channel length and a transit frequency of 135 MHz," *IEEE Trans. on El. Dev.*, vol. 60, no. 9, pp. 2815–2820, 2013. <http://dx.doi.org/10.1109/TED.2013.2274575>
- [9] H. Gummel, "On the definition of the cutoff frequency ft," *Proceedings of the IEEE*, vol. 57, no. 12, pp. 2159–2159, 1969. <https://doi.org/10.1109/PROC.1969.7509>
- [10] R. Shabanpour, T. Meister, K. Ishida, B. K. Boroujeni, C. Carta, U. Jörges, F. Ellinger, L. Petti, N. Münzenrieder, G. A. Salvatore, and G. Tröster, "Cherry-hooper amplifiers with 33 db gain at 400 khz bw and 10 db gain at 3.5 mhz bw in flexible self-aligned a-igzo tft technology," in *Intelligent Signal Processing and Communication Systems (ISPACS), 2014 International Symposium on*. IEEE, 2014, pp. 271–274. <http://dx.doi.org/10.1109/ISPACS.2014.7024466>
- [11] L. Petti, A. Frutiger, N. Münzenrieder, G. A. Salvatore, L. Büthe, C. Vogt, G. Cantarella, and G. Tröster, "Flexible quasi-vertical in-ga-zn-o thin-film transistor with 300-nm channel length," *IEEE Electron Device Letters*, vol. 36, no. 5, pp. 475–477, 2015. <https://doi.org/10.1109/LED.2015.2418295>
- [12] N. Münzenrieder, G. A. Salvatore, L. Petti, C. Zysset, L. Büthe, C. Vogt, G. Cantarella, and G. Tröster, "Contact resistance and overlapping capacitance in flexible sub-micron long oxide thin-film transistors for above 100 mhz operation," *Applied Physics Letters*, vol. 105, no. 26, p. 263504, 2014. <https://doi.org/10.1063/1.4905015>
- [13] H. Shichman and D. A. Hodges, "Modeling and simulation of insulated-gate field-effect transistor switching circuits," *IEEE Journal of Solid-State Circuits*, vol. 3, no. 3, pp. 285–289, 1968.
- [14] H. Bae, S. Kim, M. Bae, J. S. Shin, D. Kong, H. Jung, J. Jang, J. Lee, D. H. Kim, and D. M. Kim, "Extraction of separated source and drain resistances in amorphous indium-gallium-zinc oxide tfts through c-v characterization," *IEEE Electron Device Letters*, vol. 32, no. 6, pp. 761–763, 2011. <https://doi.org/10.1109/LED.2011.2127438>
- [15] C. H. Doan, S. Emami, A. M. Niknejad, and R. W. Brodersen, "Millimeter-wave cmos design," *IEEE Journal of solid-state circuits*, vol. 40, no. 1, pp. 144–155, 2005. <https://doi.org/10.1109/JSSC.2004.837251>
- [16] V. Teppati, S. Tirelli, R. Lölblom, R. Flückiger, M. Alexandrova, and C. R. Bolognesi, "Accuracy of microwave transistor ft and fmax extractions," *IEEE Transactions on Electron Devices*, vol. 61, no. 4, pp. 984–990, 2014. <http://dx.doi.org/10.1109/TED.2014.2306573>
- [17] D. Koretomo, T. Toda, T. Matsuda, M. Kimura, and M. Furuta, "Anomalous increase in field-effect mobility in in-ga-zn-o thin-film transistors caused by dry-etching damage through etch-stop layer," *IEEE Transactions on Electron Devices*, vol. 63, no. 7, pp. 2785–2789, 2016. <https://doi.org/10.1109/TED.2016.2568280>
- [18] N. Munzenrieder, P. Voser, L. Petti, C. Zysset, L. Buthe, C. Vogt, G. A. Salvatore, and G. Troster, "Flexible self-aligned double-gate igzo tft," *IEEE Electron Device Letters*, vol. 35, no. 1, pp. 69–71, 2014. <https://doi.org/10.1109/LED.2013.2286319>
- [19] J. G. Um and J. Jang, "Heavily doped n-type a-igzo by f plasma treatment and its thermal stability up to 600 c," *Applied Physics Letters*, vol. 112, no. 16, p. 162104, 2018. <https://doi.org/10.1063/1.5007191>
- [20] H. Gleskova, S. Wagner, and Z. Suo, "a-si: H thin film transistors after very high strain," *Journal of Non-Crystalline Solids*, vol. 266, pp. 1320–1324, 2000. [https://doi.org/10.1016/S0022-3093\(99\)00944-8](https://doi.org/10.1016/S0022-3093(99)00944-8)
- [21] N. Munzenrieder, L. Petti, C. Zysset, G. Salvatore, T. Kinkeldei, C. Perumal, C. Carta, F. Ellinger, and G. Troster, "Flexible a-igzo tft amplifier fabricated on a free standing polyimide foil operating at 1.2 mhz while bent to a radius of 5 mm," in *Electron Devices Meeting (IEDM), 2012 IEEE International*, 2012, pp. 5–2. <https://doi.org/10.1109/IEDM.2012.6478982>